Online Energy Management in Microgids Considering Reactive Power

Hualei Zou, *Student Member, IEEE*, Yu Wang, *Member, IEEE*, Shiwen Mao, *Senior Member, IEEE*, Fanghua Zhang, and Xin Chen, *Member, IEEE*

***Abstract*—The optimal power energy scheduling of a Microgrid (MG) is not only related to the active power of distributed generators, but also dependent on the reactive power and system operational constraints. It is essential to manage the active and reactive power simultaneously in optimal energy distribution. This paper is focused on developing an online algorithm to optimize the real-time power energy distribution in the MG, considering both reactive power and system operational constraints. The goal is to provide high quality electricity usage for users in the MG and maximize users' utility. The output power of controllable generators are also optimized. The proposed online algorithm is asymptotically optimal, since its solution converges to the offline optimal solution. The effectiveness of the proposed algorithm is validated using data traces obtained from a real-world MG.**

***Index Terms*—Energy Management System, Smart Grid, online algorithm, power quality, Averaging Fixed Horizon Control.**

I. Introduction

The Internet of Things (IoT) is a new paradigm that consists of a pervasive presence around us of a variety of "things" or "objects." The "things" in the IoT are connected to the Internet through Radio-Frequency Identification (RFID) and other information-sensing devices [1]. They are also able to interact with each other and cooperate with their neighboring "smart" components to achieve common goals, such as enabling intelligent identification and management [2], [3]. The Smart-grid/Microgrid (SG/MG) is an important domain of the IoT, which attracts increasing attention for the high resilience and self-healing features when there exists an attack or natural disasters caused geographic area outages [4], [5]. Furthermore, SG/MG is widely studied for it is cost-efficient and environmental friendly. Generally, SG/MG adopts various IoT technologies, such as RFID, sensors, and communications to quickly capture and deliver critical signals to guarantee high resilience and resistance to various cyber attacks [4]–[6]. The real-time connections among users, power supply companies, and generators, as enabled by IoT technologies, are critical to achieve real-time, high-speed, and bi-directional flow of information and electricity [6], [7]. These can effectively improve the level of informatization of power systems, promote the efficiency of renewable energy, and enhance the stability of Smart-grid/Microgrid, which are important goals of energy management systems (EMS) [4], [8].

The EMS in the MG has four main function modules, including human-computer interaction, data analysis, prediction, and decision optimization [5], [9], [10]. The optimal decisions are made in the EMS, which can be day-ahead or in real-time. For day-ahead EMS, researchers assume that all system states over time are known *a priori*, such as load demand, renewable power generation, and electricity price. Then optimal scheduling can be achieved by solving an offline optimization problem with goals of minimizing the operation cost or energy loss, maximizing users' utility or power companies' profit, shaping the demand profile, and so on [8]–[12]. However, when the accuracy of predicted values is low, this method usually performs poorly. Thus many researchers focus on promoting the accuracy of prediction in the EMS to mitigate this problem [13]–[15]. However, perfect forecasting of the complex SG/MG information is very challenging in practice, since such systems are inherently highly random (e.g., affected by future weather conditions and random user behavior).

Another means to tackle this problem is applying stochastic programming for day-ahead EMS. Based on the probabilistic characteristics of the uncertainties, several scenarios are first obtained through Monte Carlo and scene reduction techniques. Then, deterministic optimization algorithms can be applied to solve the optimal scheduling problem [16], [17]. With this approach, the uncertainties are considered day-ahead; however, it still requires accurate information on the probability distribution of uncertainties, which could be difficult to obtain. This approach usually incurs high computational complexity.

To make the optimal power distribution adaptive to real-time variations in the SG/MG environment, online optimization algorithms have been recognized to be highly promising for real-time MG energy scheduling, which only rely on real-time information or very-short-time-ahead predictions (which are usually highly accurate) [18]. The optimal controls, decisions, output generation, consumption level, and the utility gained by this method are usually closer to the actual situation, and the information is sent to distributed generators and customers in a timely fashion [19]–[21].

Many existing online algorithms for MG energy management are asymptotically optimal, i.e., their solution converges to the offline optimal solution although they do not require future information [19]–[21]. However, these existing works

This work is supported by the National Natural Science Foundation of China under Grants No. 51607087 and No. 51377079, the Fundamental Research Funds for the Central Universities of China NO. XCA17003-06, in part by the NSF under Grant DMS-1736470, and by the Wireless Engineering Research and Education Center at Auburn University.

H. Zou, Y. Wang, F. Zhang, and X. Chen are with the Department of Electrical Engineering, Nanjing University of Aeronautics and Astronautics, Nanjing, Jiangshu 210016, China. S. Mao is with the Department of Electrical and Computer Engineering, Auburn University, Auburn, AL 36849-5201, USA. Email: zouhualei@nuaa.edu.cn, yuwang15@nuaa.edu.cn, smao@ieee.org, zhangfh@nuaa.edu.cn, chen.xin@nuaa.edu.cn. Y. Wang is the corresponding author.

only consider the balance of the supply and demand of active power in the MG. Several other important aspects, including the actual power laws (e.g., Kirchhoff's laws) and system operational constraints (e.g., voltage stable range) have not been fully considered. Consequently, the optimal control strategies on power flow and output generation achieved by these algorithms may violate the actual system constraints. A real-word MG should operate stably and always provide high quality electricity to users. It is essential to develop a comprehensive problem formulation that takes into account all the important aspects of the MG, as well as effective solution algorithms with low computational complexity (for real-time operation of the MG) and optimal performance.

In this paper, we focus on developing an online algorithm for the MG EMS to achieve optimal energy scheduling, which takes into account both actual power laws and system operational constraints. We formulate the online energy distribution as an optimal power flow (OPF) problem with multi-objective. The objectives of our problem formulation include maximizing uses' utility, providing high quality electricity for users all the time, optimizing the output power of controllable generators in the MG system, and keeping the system operating in an economic style. To solve the online optimal MG energy distribution problem, Receding Horizon Control (RHC) has been successfully applied in prior work [20], [22], [23]. The essence of this method is to replace the process of solving a static large-scale model optimization problem by solving a series of small-scale optimization problems, which can effectively reduce the computational complexity and adapt to the time-varying environment. However, these prior works assume prefect prediction of future events in a fixed operational time window, but ignores future updates on prediction [20], [22] . They also assume that the uncertainties of renewable power and load demand are independent [23]. These assumptions may be strong in a real-world MG system. To address these issues, we propose to employ Averaging Fixed Horizon Control (AFHC) [24], [25] to solve our online optimal MG energy distribution problem, which only makes some mild assumptions on the uncertainties in renewable power and load demand, and these assumptions are exactly inline with the real-world situation.

The objective function of the formulated problem is convex but non-differentiable [26]. The constraints are based on the physical power system, considering all the key operational features, but are non-convex [27], [28]. To solve this challenging problem, we first apply equivalent transformations to make the objectives differentiable and convex, which, however, still have the same optimal solution as the original problem [29]. Then the slacking method is applied to transform the non-convex feasible set to convex [30]. Then our online energy scheduling scheme is converted to a convex problem, and solved with the semidefinite programming (SDP) based interior point method. We prove that the energy schedule achieved by our online algorithm is asymptotically optimal, since it converges to the offline optimal solution. To validate the performance of the proposed scheme, we apply it to a real-world MG deployed in Hekou, Nantong City, Jianshu Province, China. Our simulation study shows that the online schedule converges to the offline optimal solution in expectation. Furthermore, users can enjoy high-quality electrical energy in our system even when the real power of renewable resources and load demand fluctuate rather violently. Finally, the output power of controllable generators is optimized and the voltage at every bus in the MG is maintained within the allowed tolerance range.

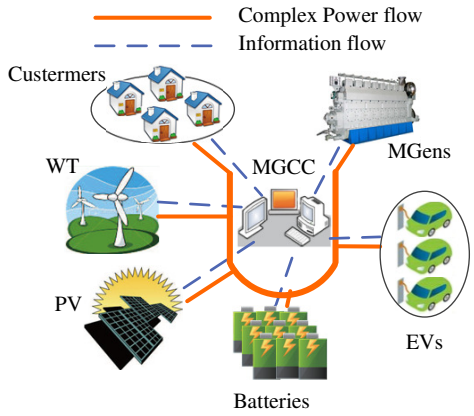

Fig. 1. System architecture of a Microgrid.

The remainder of this paper is organized as follows. We present the system model and problem statement in Section II. The proposed online algorithm is developed and analyzed in Section III. The simulation, validation, and evaluation of our proposed algorithm are represented in Section IV. Section V concludes this paper.

II. System Model and Problem Formulation

A. System Model

We consider an MG integrated with renewable resources, energy storage system (ESS), Micro-generators (MGENs), load demand, and an MG control center (MGCC) as shown in Fig. 1. The renewable energy sources in the MG include photovoltaic (PV), wind turbine (WT), and so on. The energy consumption in the MG can come from residential, commercial, and industrial consumers. Such loads are usually divided into two types [31], [32]. One type is fixed load, such as refrigerators in houses and manufacturing machines in factories. The other is elastic loads, such as electric vehicles (EVs), HVAC (heating, ventilation and air conditioning), and washer/dryers, which can be flexibly scheduled in the MG. In AC MG, many loads are induction motors, and both the active and reactive power demands are satisfied in the system. The MGCC gathers information from local controllers (LCs), receives the optimal energy strategies from the EMS, and then sends the corresponding control commands to the LCs.

The Energy Management System (EMS) in the MG is used to achieve optimal energy distribution. The MGCC collects renewable power, users' load demand, the upper and lower limits of MGENs's active/reactive power and voltage in each node through communications links. Then the optimal scheduling information will be sent to the generators side and the consumer side, respectively. Both complex power and information flow bidirectionally in the MG system.

Moreover, the ESS charges the extra power and discharges when the demand is larger than DG's generation. The elastic

TABLE I
NOTATION

Symbol	*Description*
T	the time period of one round
t	time slot, $t = 1, 2, ..., T$
i, j	the buses in the power system
e, f	the real, imaginary parts of voltage
P	the real/active power in the power system
Q	the reactive power in the power system
Structure parameters	
$G_{i,j}$	the conductance between node i and j
$B_{i,j}$	the susceptance between node i and j
$\alpha_{d,t}$	the quadratic coefficient of diesel d at time t
$\alpha_{s,t}$	the quadratic coefficient of battery d at time t
$\beta_{d,t}$	the linear coefficient of diesel d at time t
$\lambda_{d,t}$	the constant coefficient of diesel d at time t
η	the diesel's smoothing coefficient
ω	the prediction window size
$C_{d,t}$	the cost of all diesels at time t
$C_{s,t}$	the cost of all batteries at time t
Variables	
$P_{l,t}$	the active power of fixed load demand at time t
$P_{e,t}$	the active power of elastic load demand at time t
$P_{r,t}$	the active power of renewable power at time t
$P_{d,t}$	the active power of diesel's output power at time t
$P_{s,t}$	the active power of battery's output power at time t
$Q_{l,t}$	the reactive power of load demand at time t
$Q_{e,t}$	the reactive power of elastic load demand at time t
$Q_{k,t}$	the reactive power of generator k at time t
$\rho_{r,t}, \rho_{s,t}, \rho_{d,t}$	the efficiency of the converters connected to the PV array and ESS, and the power loss in MGENs at time t
e_i, f_i	the real and imaginary part of voltage at node i
e_{ref}, f_{ref}	the real and imaginary part of voltage at reference node
$\mu_{d,t}, \upsilon_{d,t}$	the transformation variables of $P_{d,t}$
Ω, ω	the variables to relax the upper/lower bounder of active power from inequality to equation
Δ, δ	the variables to relax the upper/lower bounder of reactive power from inequality to equation
Λ, ζ	the variables to relax the upper/lower bounder of voltage from inequality to equation
$P_{net,t}$	the net active power demand at time t
$SoC_{s,t}$	the battery s state of charge at time t
ξ, γ	the auxiliary variables for real and reactive power
o^{max}, o^{min}	the upper, lower bound of variables
$\hat{v}$	the predictive value of v
$\bar{v}$	the average value of v
$b_{d,t}$	the binary variables to relax $P_{d,t}$ in absolute value term at time t
Sets	
$\mathbb{B}$	the set of buses
$\mathbb{D}, \mathbb{S}, \mathbb{E}$	the set of diesels, ESS and elastic load
$\mathbb{K}$	the set of reactive power sources

load is also one of the effective ways to consume excess energy to keep the supply-demand balance and maximize the use of renewable resources. Furthermore, reactive power resources, such as ESS, MGENs, SVC (static var compensator), are regulated to avoid voltage fluctuations at each node that are caused by the intermittent power of the renewable generation and load demand.

On the basis of realizing stable operation of the system, the EMS can achieve maximum user satisfaction for electricity usage in the MG. The system can operate in an economic way, and the optimal output power of the adjustable power generation can be achieved.

In this paper, d denotes the real power output of the MGEN, $d \in \mathbb{D} = \{1, 2, ..., D\}$, and $\mathbb{D}$ is the set of all MGENs in our MG. We define the set of active powers of ESS as $s \in \mathbb{S} = \{1, 2, ..., S\}$; and the elastic load is represented as $e \in \mathbb{E} = \{1, 2, ..., E\}$. The set of real power resources $\mathbb{G}$ is constituted by $\mathbb{D}$, $\mathbb{S}$ and $\mathbb{E}$. For reactive power generators, we assume the set is $\mathbb{K}$, and $k \in \mathbb{K} = \{1, 2, ..., K\}$. Actually, distributed energy scheduling is related to the structure parameters in the MG. In our system, the set of buses is $\mathbb{B}$, and $i, j \in \mathbb{B} = \{1, 2, ..., B\}$. The notation used in this paper is summarized in Table I.

B. Problem Formulation

In our system, the active load demand is $P_{l,t}$ at time t. Correspondingly, the reactive power demand is $Q_{l,t}$. In order to maximize the output power of renewable resources, renewable generators output their maximum active power, and they are the uncontrollable generators in the MG. Taking into account the efficiency of the converters connected to the PV array and ESS, and the power loss in MGENs (let their efficiency be $\rho_{r,t}$, $\rho_{s,t}$, and $\rho_{d,t}$), the real output powers of renewable generators, ESS and MGENs are $\rho_{r,t}P_{r,t}$, $\rho_{s,t}P_{s,t}$, $\rho_{d,t}P_{d,t}$, respectively.

For an MG, user's electricity demand, the fixed load $P_{l,t}$, should be satisfied at every time, and the elastic load $P_{e,t}$ should be adjusted flexibly. In this paper, we maximize users' utility by coordinating the complex power generation in the MG [33] and optimizing the operation of MGENs according to their output features [34], [35]. The cost of the MG is mainly on the MGENs and ESS, and we assume the costs of MGENs and ESS are limited [19]. To achieve the above goals, we formulate the power energy scheduling problem as follows.

$$\min: \sum_{t=1}^{T} \left\{ \left[P_{l,t} + P_{e,t} - (\rho_{d,t}P_{d,t} + \rho_{s,t}P_{s,t} + \rho_{r,t}P_{r,t})\right]^2 + \sum_{d=1}^{D} \eta |P_{d,t} - P_{d,t-1}| \right\} \tag{1}$$

$$\text{s.t.:} \sum_{d=1}^{D} (\alpha_{d,t}P_{d,t}^2 + \beta_{d,t}P_{d,t} + \lambda_{d,t}) \leq C_{d,t} \tag{2}$$

$$\sum_{s=1}^{S} \alpha_{s,t}P_{s,t}^2 \leq C_{s,t}. \tag{3}$$

In probelm (1), the objective consists of two major items: the first one is to minimize the users' dissatisfaction, and the second item is to minimize the fluctuation in the output of MGENs, where η is the optimal coefficient. Furthermore, $P_{d,t}$ and $P_{d,t-1}$ are the MGENs' real power output at time t and $t-1$, respectively, and $P_{d,0} = 0$; $C_{d,t}$ and $C_{s,t}$ are the upper bounds on the costs of MGENs and ESS at time t, respectively; $\alpha_{d,t}$, $\beta_{d,t}$, and $\lambda_{d,t}$ are the cost coefficients of MGENs; and $\alpha_{s,t}$ is the cost coefficient of ESS.

In addition to satisfying the balance of supply and demand of active power in MG, there are usually many inductive loads in the AC MG system. Therefore, the reactive power

must be considered simultaneously. Furthermore, the balance of active and reactive power is related to the bus voltages and the structural parameters between interconnected nodes. Therefore, the system's stable operation constraints should include:

(i) Power flow constraints:

$$\begin{cases} P_{g,i} - \sum\limits_{j\in\mathbb{B}}[e_i(e_jG_{ij} - f_jB_{ij}) + f_i(f_jG_{ij} + e_jB_{ij})] = P_{li} \\ P_{d,i} - \sum\limits_{j\in\mathbb{B}}[e_i(e_jG_{ij} - f_jB_{ij}) + f_i(f_jG_{ij} + e_jB_{ij})] = P_{li} \\ Q_{k,i} - \sum\limits_{j\in\mathbb{B}}[f_i(e_jG_{ij} - f_jB_{ij}) - e_i(f_jG_{ij} + e_jB_{ij})] = Q_{li}, \end{cases}$$
$$g \in \mathbb{G}/\mathbb{D}, i \in \mathbb{B}, d \in \mathbb{D}, k \in \mathbb{K}, \forall t, \tag{4}$$

where $Q_{k,i}$ is the reactive power output at time t for reactive generator k; e_i and f_i are the real and imaginary part of voltage at bus i, respectively; P_{li} and Q_{li} are the active and reactive power demand at bus i, respectively; G_{ij} and B_{ij} are the conductance and susceptance between nodes i and j, respectively. Constraint (4) aims to achieve the supply-demand balance in both real and reactive power, and this balance is related to the voltage of each bus and structure parameters in the MG.

(ii) Limits of active and reactive power, and of the ESS capacity:

$$\begin{cases} P_d^{min} \le P_{d,i} \le P_d^{max}, \ \forall t \\ P_g^{min} \le P_{g,i} \le P_g^{max}, \ \forall t \\ Q_k^{min} \le Q_{k,i} \le Q_k^{max}, \ \forall t \\ SoC_{s,t} = SoC_{s,t-1} - \eta_s P_{s,t}, \ \forall t \\ SoC_s^{min} \le SoC_{s,t} \le SoC_s^{max}, \ \forall t, \end{cases} \tag{5}$$

where x^{max} and x^{min} are the upper and lower limits of variable x. $SoC_{s,t}$ is the state of charge for ESS at time t. During the optimal operation period, it should be within the ESS capacity at any time. $P_{s,t}$ is negative when the ESS is charging and positive when the ESS is discharging. η_s is the charge/discharge efficiency of the ESS. Constraint (5) is used to ensure all generators run in the safety ranges of the real power and reactive power resources. This is very important to achieve stable operation in the MG.

(iii) In order to keep the voltage of each bus in the MG within the stable range, we enforce limits on the voltage amplitude at each bus and the reference bus, as

$$\begin{cases} (V_i^{min})^2 \le (e_i^2 + f_i^2) \le (V_i^{max})^2, \ \forall t \\ e_{ref}^2 = e_0^2, \ \forall t \\ f_{ref}^2 = f_0^2, \ \forall t, \end{cases} \tag{6}$$

where e_{ref} and f_{ref} are the real and imaginary part of voltage in the reference bus, respectively. Generally, one MGEN is chosen as the slack generator.

C. Problem Decomposition based on Time Windows

1) Assumptions on Predictions: It can be seen from (1) to (6) that if the optimal scheduling is calculated just by the forecast information, then these results often cannot be used directly. This is because there is always a deviation between the predicted and the actual values of the PV power and load demand. Therefore, some assumptions need to be declared to make the optimal energy distribution more instructive to the actual scheduling. In our system, we have some assumptions on renewable power and users' load demand before solving the optimization problem. And these assumptions on predictions serve as the middle ground between the worse-case and the stochastic viewpoints [24].

The relationship between the actual value and predicted value of renewable power $P_{r,t}$ and load demand $P_{l,t}$ are established as:

$$\begin{cases} P_{l,t} = \hat{P}_{l,t} + \sum_{z=1}^{t} f_l(t-z)e_l(z) \\ P_{r,t} = \hat{P}_{r,t} + \sum_{z=1}^{t} f_r(t-z)e_r(z), \end{cases} \tag{7}$$

where $\hat{P}_{l,t}$ and $\hat{P}_{r,t}$ are the predictions of $P_{l,t}$ and $P_{r,t}$, respectively, made at time $z < t$. Thus, it can be seen that the prediction error $\sum_{z=1}^{t} f(t-z)e(z)$ is modeled as a weighted linear combination of previous-step noise terms (i.e., $e(z)$). We assume that the noise terms are independent and identically distributed (i.i.d.) with mean zero and positive definite covariance Re; and that the weight function $f(\cdot)$ satisfies $f(0) = I$ and $f(t) = 0$ for $t < 0$. Furthermore, it is common for the impulse function to decay as $f(z) \sim 1/z^{\sigma}$. The forecast value can be updated with time passes according to (7). This assumption is closer to the actual situation.

2) Averaging Fixed Horizon Control Algorithm: In the objective function (1), the second term is to achieve a smooth control on the output power of the MGENs. It can be seen that global information must be obtained in order to solve the problem, due to the coupling of MGENs' output powers in time series. However, Eq. (7) indicates that when the prediction horizon is increased, the quality of forecasts on $P_{l,t}$ and $P_{r,t}$ decline in our system. An effective way to resolve this contradiction is to adopt the RHC algorithm to achieve online optimization [36], so that in every fixed horizon window, the accuracy of renewable power and load demand is relatively high, and the goal of smoothing the output power of MGENs can be achieved.

However, the optimal results calculated by the RHC are not good enough for online optimization [25]. To this end, a promising new algorithm, termed Averaging Fixed Horizon Control (AFHC) can achieve asymptotically optimal values from predictions compared with the offline optimization algorithm [24]. In this paper, we employ AFHC to develop an online algorithm for solving the MG optimization problem; and show that the optimal scheduling calculated by this online algorithm is asymptotically convergent to the offline optimal solution. We will derive the conditions for this algorithm to achieve the offline optimal in III-C.

Let the active power be $P_t = [P_{d,t}, P_{s,t}, P_{e,t}]^T$ and the window size of the AFHC be $(w+1)$. Every set in each window is defined as: $\Psi_m = \{i : i \equiv m \ \text{mod}(w+1)\} \cap [-w, T], m = 0, 1, ..., w$. To simplify notation, we define $\hat{h}_t(P_t) = (P_{l,t} + P_{e,t} - (\rho_{d,t}P_{d,t} + \rho_{s,t}P_{s,t} + \rho_{r,t}P_{r,t}))^2$, so the optimization problem in the mth window becomes:

$$\begin{aligned} \min \ & \sum_{t=\tau}^{\tau+w} \left(\hat{h}_t(P_t) + \sum_{d=1}^{D} \eta |P_{d,t} - P_{d,t-1}| \right) \\ \text{s.t.:} \ & (2) \sim (6), \ \tau \in \Psi_m. \end{aligned} \tag{8}$$

Let $(P_{FHC}^{(k)})_{t=z}^{z+w}$ represent the solution to (8), and $P_{FHC,t}^{(k)} = 0$ when $t \leq 0$. Then for $(w+1)$ versions of FHC, AFHC can be obtained by averaging the solutions of $(w+1)$ FHC algorithms, i.e., $P_{AFHC,t} = 1/(w+1) \sum_{m=0}^{w} P_{FHC,t}^{m}$.

III. Solution Algorithm

Through the analysis of the mathematical model in Sections II-B and II-C, it can be seen that the objective function for smooth control of the MGEN output power is convex but non-differentiable, which poses a computational challenge than solving a differentiable function [26]. In addition, as in Section II-B, in order to ensure stable operation of the MG system, the reactive power in the system must be coordinated. However, due to the introduction of reactive power, the optimal analytic set is not convex anymore [27], [28]. Traditional convex optimization techniques cannot be used to solve this problem. To address these challenges, we propose an online algorithm in this section. We will show that our online algorithm is asymptotically convergent to the offline optimal solution, and has a sublinear regret, i.e., the online solution is equivalent to the offline optimal solution in expectation. We will derive the conditions for the proposed online algorithm to achieve these excellent properties in Section III-C, and present the pseudocode of the online algorithm in Section III-D.

A. Transformation of the Objective Function

In our formulation, the objective function is convex but not differentiable. Therefore, it is necessary to carry out an equivalent transformation for the mathematical model of the smooth term. We adopt the method in [29]; we introduce binary variables $b_{d,t}$ to transform (1). The problem is then equivalent to:

$$\begin{aligned}
\min\ & \sum_{t=\tau}^{\tau+w} [P_{net,t} - (\rho_{d,t} P_{d,t} + \rho_{s,t} P_{s,t} - P_{e,t})]^2 \qquad (9)\\
& + \sum_{d=1}^{D} \eta \left(b_{d,t}(P_{d,t} - P_{d,t-1}) - (1 - b_{d,t})(P_{d,t} - P_{d,t-1}) \right)\\
\text{s.t.: } & (2) \sim (6)\\
& b_{d,t}(P_{d,t} - P_{d,t-1}) \geq 0,\ \forall t\\
& (1 - b_{d,t})(P_{d,t} - P_{d,t-1}) \leq 0,\ \forall t\\
& b_{d,t} \in \{0, 1\},\ \forall t,
\end{aligned}$$

where $P_{net,t} = P_{l,t} - \rho_{r,t} P_{r,t}$ is the net power demand in the MG. Note that this transformation is equivalent to the original objective. However, it introduces the binary variables, while the optimization problem is still hard to solve. Thus, further transformations are necessary. We next define $\mu_{d,t} = b_{d,t} P_{d,t}$ and $\upsilon_{d,t} = (1 - b_{d,t}) P_{d,t}$, and then (9) is transformed to:

$$\begin{aligned}
\min\ & \sum_{t=\tau}^{\tau+w} [P_{net,t} - (\rho_{d,t}(\mu_{d,t} + \upsilon_{d,t}) + \rho_{s,t} P_{s,t} - P_{e,t})]^2\\
& + \sum_{d=1}^{D} \eta(\mu_{d,t} - \upsilon_{d,t} - (\mu_{d,t-1} + \upsilon_{d,t-1})) \qquad (10)\\
\text{s.t.: } & (2) \sim (6)\\
& \mu_{d,t} - \mu_{d,t-1} \geq 0,\ \forall d, \forall t\\
& \upsilon_{d,t} - \upsilon_{d,t-1} \leq 0,\ \forall d, \forall t\\
& \mu_{d,t} \cdot \upsilon_{d,t} = 0,\ \forall d, \forall t,
\end{aligned}$$

where $\mu_{d,0} = 0$ and $\upsilon_{d,0} = 0$ in our system.

According to Lemma 2.1 in [29], the nonlinear equality constraints in (10) are redundant in the actual optimization solution. Thus (10) can be further simplified to:

$$\begin{aligned}
\min\ & \sum_{t=\tau}^{\tau+w} [P_{net,t} - (\rho_{d,t}(\mu_{d,t} + \upsilon_{d,t}) + \rho_{s,t} P_{s,t} - P_{e,t})]^2\\
& + \sum_{d=1}^{D} \eta(\mu_{d,t} - \upsilon_{d,t} - (\mu_{d,t-1} + \upsilon_{d,t-1})) \qquad (11)\\
\text{s.t.: } & (2) \sim (6)\\
& \mu_{d,t} - \mu_{d,t-1} \geq 0,\ \forall d, \forall t\\
& \upsilon_{d,t} - \upsilon_{d,t-1} \leq 0,\ \forall d, \forall t.
\end{aligned}$$

With the above transformations, the optimal energy distribution in (11) is the same as that in (8). Theorem 1 summarizes the condition to achieve this result. The proof of Theorem 1 is presented in Appendix A.

Theorem 1. *If $\eta > 0$, an optimal solution to problem (11) is also optimal to problem (8). That is, the optimal active power output of the distributed power generation in the MG solved by (11), $P_t^* = [P_{d,t}^*, P_{s,t}^*, P_{e,t}^*]^T$, is also the optimal scheduling solved by the original problem (8).*

Through the above transformations, the original objective function (8) becomes (11), which is a differentiable and convex function and is much easier to solve.

B. Convex Relaxation of the OPF Constraints

Through the above equivalent transformation analysis, the objective function becomes a continuous, differentiable function. However, due to the regulation on the reactive power to keep the voltage at each bus within stable range, the feasible set constituted by system's constraints is a typical non-convex set. The problem is thus a non-convex problem and NP-hard to solve [27], [30]. Therefore, an appropriate transformation must be performed on this feasible set as well.

For online optimization of the MG, the solution algorithm should be fast for real-time operation. To this end, semidefinite programming (SDP) based interior point method has the major advantage of avoidance of deriving and computing the Jacobian matrices and the Hessian matrices for each problem, which helps to effectively improve the algorithm speed [30]. Thus we adopt SDP relaxation in this section. All the constraints are transformed into quadratic equality

by introducing auxiliary and slack variables. This way, we transform the classical OPF problem into SDF, and the detailed transformation is shown in Appendix B. After slacking, the feasible set becomes convex.

C. Online Optimization Indicator and Conditions

In this section, the AFHC method is employed to develop an online algorithm for solving the MG scheduling problem. The online algorithm solution converges asymptotically to the offline optimal solution. To evaluate the performance of the algorithm, here we define the online optimization as:

$$C_{on} = \sum_{t=1}^{T} \left(\hat{h}(P_t) + \sum_{d=1}^{D} \eta |P_{d,t} - P_{d,t-1}| \right), \quad (12)$$

where C_{on} denotes the online result and $P_{d,0} = 0$. Correspondingly, the static offline optimization is:

$$C_{off} = \arg\min_{P_t} \sum_{t=1}^{T} \left(h(P_t) + \sum_{d=1}^{D} \eta |P_{d,t} - P_{d,t-1}| \right), \quad (13)$$

where C_{off} is the offline optimization result and $P_{d,0} = 0$.

For the AHFC based online optimization algorithm, if the predicted renewable output power $\hat{P}_{r,t}$ and load demand $\hat{P}_{l,t}$ satisfy assumption (7) in Section II-C and the predicted net power $\hat{P}_{net,t}$ satisfies condition (14), we have

$$\inf_{\hat{P}_{net,t}} \left\{ \mathbb{E}_e \left\{ \sum_{t=1}^{T} \sum_{n=1}^{N} \left(AA^{\dagger} \left(P_{net,t} - \frac{1}{T} \sum_{t=1}^{T} P_{net,t} \right) \right)^2 \right\} \right\} \geq \varepsilon T, \quad (14)$$

where $A = [\rho_{d,t}, \rho_{d,t}, \rho_{s,t} - 1]^T$, $A^{\dagger}$ is the Moore-Penrose pseudoinverse of A, ε is a constant when w, Re, and η, A is known; and $\varepsilon = f(Re, w)$. Here Re affects the convergence speed of the online optimization to the offline optimal energy scheduling, but it does not affect the final convergence result. According to [24], the AFHC algorithm is strictly convergent, i.e., the following formulation holds true.

$$\sup_{\hat{P}_{l,t}, \hat{P}_{r,t}} \{ \mathbb{E}_e \{ C_{online} - C_{offline} \} \} \leq \phi(T), \quad (15)$$

and $\phi(T)$ will be 0.

D. The Proposed Online Algorithm

Base on the above analysis, we now present the online algorithm for power energy distribution in the MG. The online algorithm is presented in Algorithm 1.

Algorithm 1: Online Algorithm

Step 1: Initialize $P_0 = 0$; set the window size w;
Step 2: Set $\Psi_m = \{i : i \equiv m \mod (w+1)\} \cap [-w, T]$, $m = 0, 1, ..., w$, and then set $t = 1$ and $m = 0$;
Step 3: For $\tau \in \Psi_m$, and then for $t = \tau, \tau+1, ..., \tau+w$, update the renewable power and load demand as (7) in the entire window, defined as $\{P_{r,t}\}_{t=\tau}^{\tau+w}$ and $\{P_{l,t}\}_{t=\tau}^{\tau+w}$;
Step 4: Solve the power energy distribution problem given in (21)∼(43) to derive solution $\{P_{FHC,t}^{(m)}\}_{t=\tau}^{\tau+w}$, then

$$P_{AFHC,t} = \frac{1}{w+1} \sum_{m=0}^{w} P_{FHC,t}^{m}; \quad (16)$$

Step 5: Set $m = m + 1$ and $t = t + 1$;
Step 6: If $m \geq w$, reset $m = 0$; if $t \leq T$, go to Step 3; otherwise, end.

In Section III-C, we discuss the condition of convergence for our algorithm, and show the bound of difference in online and offline results in (15) is related to window size w. If the error of prediction is independent (i.e., error is i.i.d noise), w can be entire time horizon T, otherwise it is less than T and a finite constant according to the Corollary 6 in [24]. Thus, in (15), the time-average loss of the online algorithm goes to zero as T grows when it satisfies above conditions. This means the AHFC algorithm solution for online energy scheduling in the MG asymptotically converges to the offline optimal solution. Besides, the proposed algorithm needs to repeat T times loop for the whole operation from Step 3 to 5. In Step 4, the $\{P_{FHC,t}^{(m)}\}_{t=\tau}^{\tau+w}$ is calculated by solving SDP with polynomial time [29], [37]. Therefore, the running time of our algorithm can be obtained, which is recorded as T multiplied by a polynomial. For Algorithm 1, T is a constant, so the time complexity of our online algorithm is polynomial as well.

IV. Simulation Study and Discussions

The performances of proposed online optimal algorithm for MG scheduling are evaluated in this section by applying it to a real MG system. We first present the specific parameters and configuration of the real MG system in Section IV-A. The convergence performances of the optimal online scheduling under different conditions are examined in Section IV-B. The last Section IV-C is focused on the online scheduling performance considering reactive power.

A. Configuration and Parameters of the MG System

For performance evaluation, we consider a real-world MG system deployed in the Hekou town, Nantong City, Jianshu Province, China (GPS coordinates are $32.49°N, 120.83°E$), which consists of PVs, diesel generator, a battery energy storage system, fixed load demand, and elastic load, as shown in Fig. 2. The detailed parameters of this system are presented in Table II, where DU represents the distributed unit in the MG, IC denotes the inverter capacity, AU/AL are the upper/lower limits for the active power output, and RU/RL are the upper/lower bounds for reactive power output. The capacity of the ESS is 100kVA/250kWh. The type of diesel used in this system is VOLVO-TAD751GE, and the rated output power of the generator is 120 kW. The efficiencies of the PV and the ESS inverter are 0.96 and 0.97, respectively, and the diesel's output efficiency is 0.91 in this system.

The PV's power profile is shown in Fig. 3, where the orange curve indicates the PV power output in a sunny day and the brown curve is the PV power generation in a cloudy day. The fixed load demand in our system is mainly from the canteen

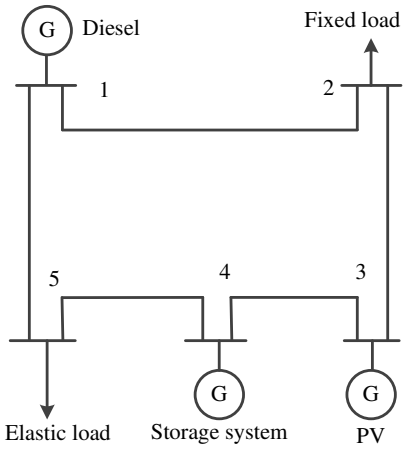

Fig. 2. Configuration of the real-world MG system deployed in the Hekou town, Nantong City, Jianshu Province, China.

TABLE II
DISTRIBUTED CAPACITY PARAMETERS IN THE MG

DU	IC (kVA)	AU (kW)	AL (kW)	RU (kVar)	RL (kVar)
Diesel	—	120	0	150	-150
Battery	300	50	-55	250	-250
Elastic load	—	40	0	30	0
PV	100	90	0	45	-45

and water pumps in a factory in town. The elastic load is mainly from air conditioners. The load profile is shown in Fig. 4. We can see that there are three load peaks which correspond to the cooking times in the morning, at noon, and in the evening, respectively.

For online optimization of power scheduling, the operation can be performed every 2 h, 1 h, 0.5 h, or 15 min. The actual timescale of operation is varied according to users' power demand. In this paper, the parameter for the AFHC is set to 30 minutes, as one window size in the MG. For the proposed online algorithm, during simulation, we run the proposed online algorithm for one day, and set the time interval in the model to 5 min. Therefore there are $T = 288$ time intervals in total.

All the simulations are executed in Matlab to verify the proposed online optimal algorithm. The SDPA-M Toolbox [38] is used to solve the reformulated SDP problem (21)∼(43). It only takes 0.04s to solve the reformulated SDP to compute the optimal energy schedule, which fully satisfies the requirements for online optimization and real-time control of the power system. The optimization method proposed in this paper is not only highly effective for the IEEE-5 system. For island-based MG, we also applied the proposed online algorithm to IEEE-14, IEEE-30, and IEEE-39 in our simulations, to validate the proposed online algorithm. We also compare the proposed online algorithm with the widely used power flow optimization solution toolbox Matpower [39]. We find the method proposed in this paper is far superior to Matpower with respect to timeliness. The detailed comparison results are presented in Table III. The simulation study shows that our proposed algorithm is highly suitable for solving the MG online optimization problem. Furthermore, our algorithm also

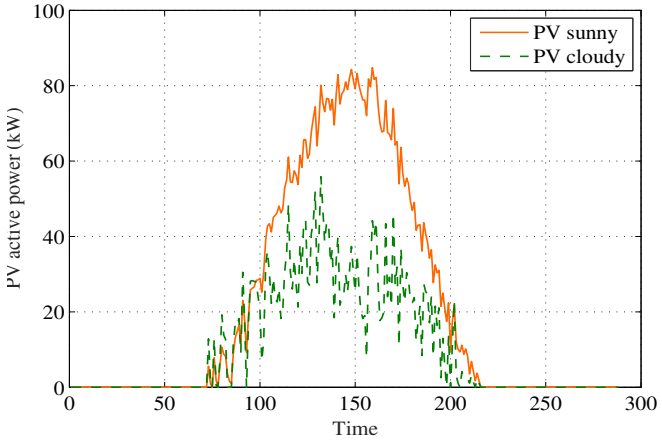

Fig. 3. PV active power in different weather.

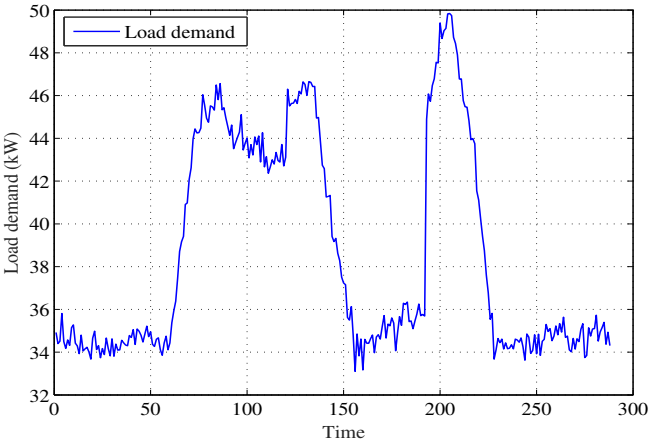

Fig. 4. Load demand in the MG.

exhibits excellent performance in convergence. The detailed simulation results are presented and discussed in the rest of this section.

B. Performance Evaluation

In order to evaluate the performance of the proposed online algorithm, we formulate the following optimal offline algorithm that minimizes the objective C_{off} over the entire time horizon T as (17).

$$\begin{aligned} \min \quad & C_{off} \\ \text{s.t.:} \quad & (22) \sim (43). \end{aligned} \tag{17}$$

We consider three cases with different features to test the convergence of the proposed online algorithm. The first case is a sunny day with high-accuracy predictions of both PV power and load demand. The second case is a sunny day with moderate-accuracy prediction of both PV power and load demand. The third case is a cloudy day with low-accuracy predictions of PV power. Generally, the prediction accuracy of PV power is relatively high when the weather is fine, with a low standard deviation in prediction error, while the factors affecting the output power of PV are more complicated when the weather is cloudy. Under bad weather,

TABLE III
CPU TIME FOR FOUR TEST SYSTEMS

System	SDP (s)	Matpower (s)
IEEE-5	0.04	0.24
IEEE-14	0.105	0.518
IEEE-30	0.347	1.193
IEEE-39	0.468	1.550

TABLE IV
PARAMETERS FOR DIFFERENT CASES

Model	Std in PV	Std in Load	Time period
Case 1	3	4	288
Case 2	5	7	288
Case 3	7	4	288

the standard deviation of prediction error will be high. The specific parameter settings are given in Table IV, where Std is the standard deviation for forecast error.

The parameters in Table IV all satisfy the inequality conditions in (14). We set η to 0.2 in the objective function, and the objective value is in US Dollar (USD). We conduct the corresponding simulations with the above three cases. For Case 1 and Case 2, we plot the difference and the expected difference between the online algorithm and offline algorithm solutions in every time slot, i.e., $C_{on}(t) - C_{off}(t)$, in Figs. 5 and 6, respectively. In the figures, the blue line denotes the difference results in Case 1, and the brown dotted line shows the difference results in Case 2.

Fig. 5 shows that the difference between the online and offline solutions is very large initially at the first 6 time slots (i.e., 30 min). This is caused by the output of diesel. In the first 6 time slots, according the principle of AFHC discussed in section II-C, the controllable variables will be increased slowly. Thus in this short time period, the power output is less than the load demand. After this period, the difference in online and offline costs are reduced quickly, only to fluctuate around 0 after a few time slots. This verifies that the online cost is very close to that of the offline optimal solution.

In Fig. 5, we also find that the gap between the online and offline algorithms in Case 1 (when the PV and load demand are predicted with high accuracy) are smaller than that in Case 2 (when the predictions are less accurate). But over the entire time horizon T, we can see that the online cost converges gradually to the offline cost in expectation, as shown in Fig. 6. It can also be seen that the convergence in Case 1 is faster than that in Case 2, i.e., high prediction accuracy helps to achieve faster convergence of the online algorithm.

Similar conclusions can be seen in Figs. 7 and 8. The fluctuation of PV power is very large due to the cloudy weather, as shown in Fig. 3, and the accuracy of prediction is low. However, our proposed online scheduling algorithm still perform very well in this adverse condition. The online results converge to the offline optimal solution very quickly in expectation, as shown in Fig. 8.

The simulation results with the three cases clearly show that the expectation of the difference of online and offline solutions $\phi(T) \rightarrow 0$. In fact, even when only part of the forecast information is available on PV power and load demand, the

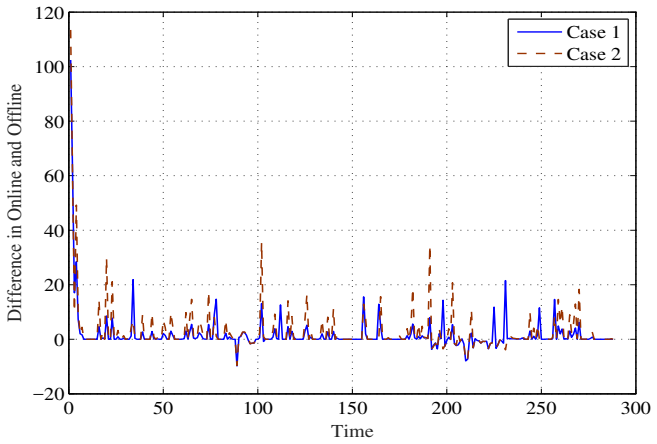

Fig. 5. The difference between the online algorithm and offline algorithm solutions over time: Case 1 and Case 2.

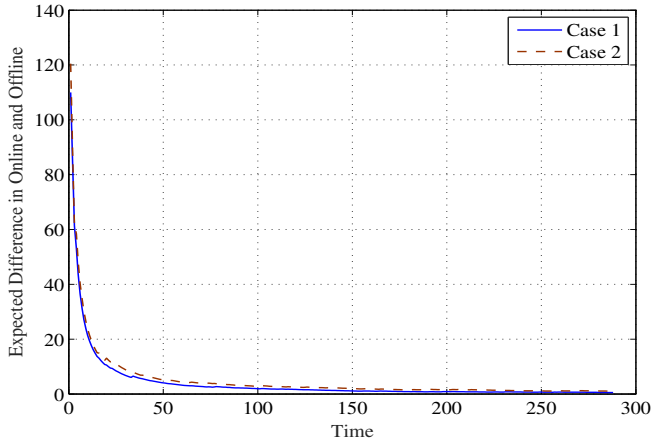

Fig. 6. The expected difference between the online algorithm and offline algorithm solutions over time: Case 1 and Case 2.

proposed online algorithm can still achieve good results as competitive as global optimization results. This is mainly due to the assumption on our prediction model in (7), which can capture the important features for real predictors. Furthermore, when we try to look ahead further into the future, the quality of predictions will get lower. This is closer to the actual forecast in PV power and load demand, and is also very different with other rolling horizon online methods which assume perfect prediction within the window and ignore the update in forecasting. Furthermore, in our model, predictions are refined over time and they are flexible enough to capture the forecast error on time series. Based of the above advantages in our model, the proposed online algorithm can achieve global optimal asymptotically. The proposed online algorithm not only achieves a good performance when the prediction accuracy is high, but also performs well when the prediction accuracy is low.

C. Online Scheduling Results Considering Reactive Power

In addition to excellent convergence performance, the AFHC in our system also performs well on smoothing the output power of the diesel, maximizing the utilization of renewable resources, and stabilizing every bus voltage. In our

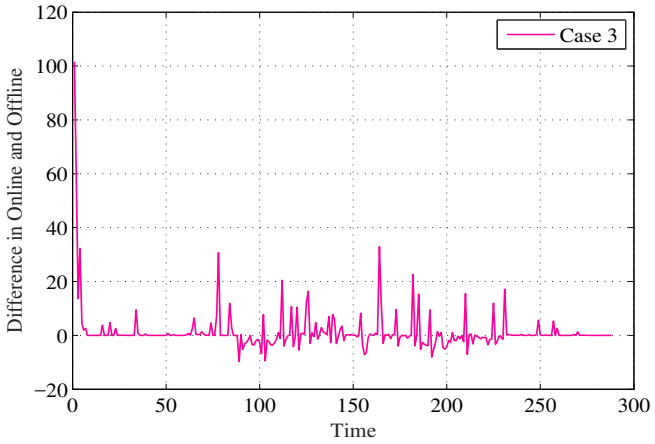

Fig. 7. The difference between the online algorithm and offline algorithm solutions over time: Case 3.

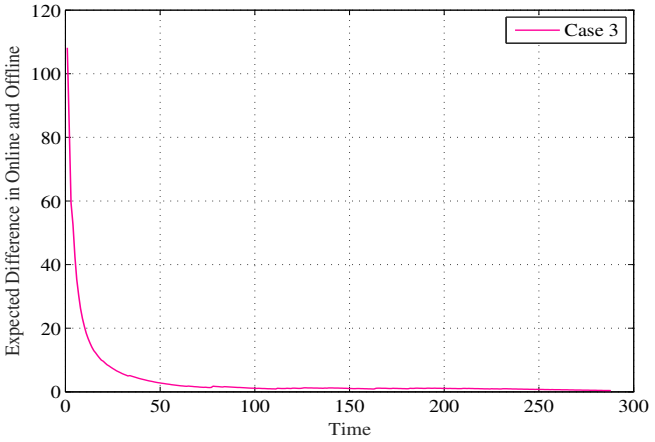

Fig. 8. The expected difference between the online algorithm and offline algorithm solutions over time: Case 3.

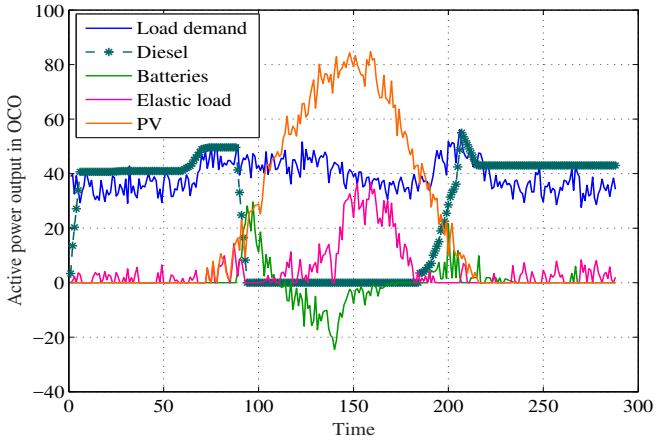

Fig. 9. Real power scheduling in the MG for Case 1.

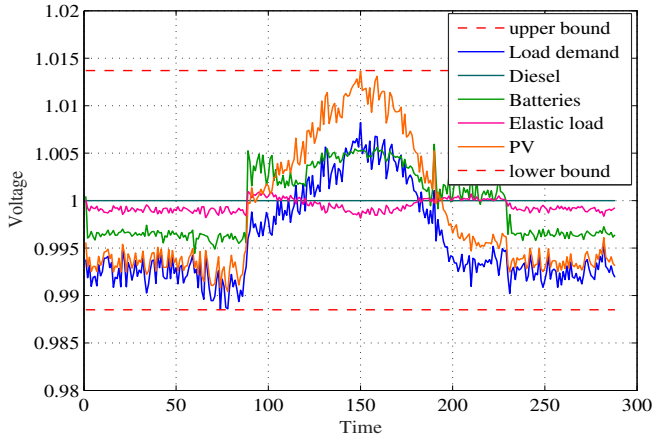

Fig. 10. Voltage in each bus in the MG for Case 1.

system, the voltage tolerances are set to be [0.95 to 1.05] p.u., which totally satisfy the requirement on low voltage power systems (e.g., voltage range [0.9 to 1.07] p.u. in China).

The detailed schedule for every micro-unit is plotted in Fig. 9 for Case 1, where the real power in every time is plotted. It can be seen that the output power of diesel increases or decreases slowly. During the time with no PV power output, elastic load is mainly coordinated to achieve the goal of smoothing the output power of diesel during time slots 7∼59 and 215∼288. At time slot 88, the PV power gradually increases. So the diesel output starts to decrease while the ESS discharges to satisfy the load demand. The diesel output power gradually decreases until time slot 94, when it reaches 0. During time slots 111∼189, the PV power is sufficient to meet the load demand. So the ESS is charged first, and then stops to work after reaching the upper limit of its capacity. Then the elastic load is fully served, which can not only balance the supply and demand of the system, but also make full use of the PV power. Fig. 9 demonstrates the effectiveness of the proposed scheme for real power distribution.

Another obvious advantage of our proposed online algorithm is that the voltage at every bus in the MG is maintained within the allowed tolerance range, which guarantees high power quality in the MG. The results are presented in Fig. 10. The red dotted lines are the upper/lower voltage bounds in our system. It can be seen from the figure that our results on bus voltages not only satisfy the requirements for MG stability, but also far exceed this requirement. Even when the real power of PV fluctuates particularly violently, the voltage at the PV bus just varies from -0.96% to 1.37% compared to the standard voltage. In the MG, the intermittent nature of the renewable resources and the fluctuation of the load demand always exist. With the proposed online optimization method, the user can enjoy high-quality electrical usage all the time.

The maximum and minimum voltages of all the buses in the MG system are also provided in Table V, which are computed in per-unit value in our system. From Table V, we find that the voltage of the diesel engine node is always equal to 1. This is because from the previous modeling, the diesel engine serves as the slack bus, i.e., the voltage of this node must remain constant during the entire operation. The voltage fluctuations at other buses are all very small. The maximum voltage deviation occurs at the PV bus, but this deviation is absolutely in line with the users' power requirements.

The above-mentioned high-quality electric energy is achieved by coordinating the reactive power in the MG, so as to ensure the voltage at each bus always operates within the allowed range. In order to illustrate the importance of reactive power in the MG, we also present the simulation results for

TABLE V
MAXIMUM AND MINIMUM VOLTAGES FOR EACH BUS IN PER-UNIT VALUE

	Diesel	ESS	Fixed load	Elastic load	PV
Maximum	1.0000	1.0059	1.0082	1.0009	1.0137
Minimum	1.0000	0.9944	0.9885	0.9981	0.9904

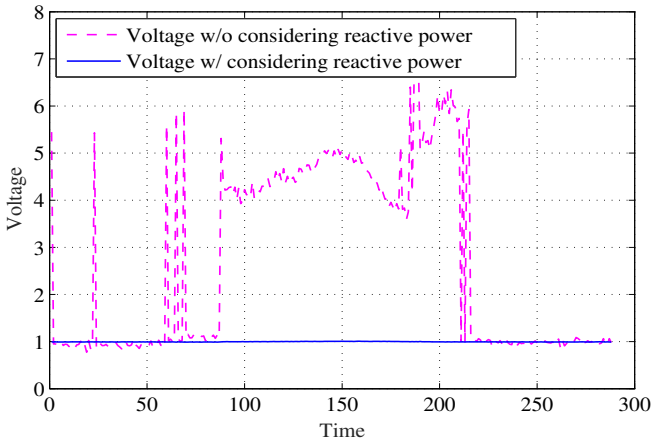

Fig. 11. Voltage in the load bus with/without considering the reactive power.

the case when the reactive resources are not considered. We find the simulated bus voltages all exceed the required range in this simulation. Since the bus voltages are similar, we take the load bus as an example, which is shown in Fig. 11. From the figure, the voltages deviate away from the allowed tolerance evidently when ignoring the reactive power in the MG. Especially when there is a fluctuation in the load demand, the voltage changes so drastically, such that the system will crash if it were the actual MG. On the contrary, the results in Fig. 10 and Table V demonstrate that our proposed optimal online algorithm can achieve the long-term objective while stabilizing the bus voltages.

Overall, the proposed online algorithm exhibits excellent performances on solving the energy distribution problem. The simulation results show that the performance of the proposed online method converges quickly to an optimal offline scheme. With AFHC, we can not only achieve effective active power scheduling, but also maintain the system voltages in a stable range by regulating the reactive power, thereby providing users with high-quality electrical energy usage, which is very important for the actual MG.

V. CONCLUSIONS

In this paper, an optimal online algorithm AFHC was proposed to solve the power energy distribution problem in the MG. Our problem formulation both maximizes users' satisfaction and minimizes the fluctuation in the MGEN output. The objective function of the formulated problem was convex but not differentiable and the feasible set was non-convex, which was hard to solve. Equivalent transformation method was employed to convert the objective function into a continuous, differentiable function. Furthermore, by introducing auxiliary variables and slack variables, we transformed the the non-convex set to convex. Finally the problem was transformed into an SDP that was easier to solve. To verify the effectiveness of our algorithm, we applied it to real-world MG. The results showed that our online algorithm asymptotically converges to the offline optimal solution. In addition, the proposed AFHC algorithm could effectively achieve the goals of smoothing the output of the diesel power and optimizing the distribution of energy. The importance of reactive power to the stable operation of the MG is also verified in our simulation study.

APPENDIX A
PROOF OF THEOREM 1

Proof: Since $P_t \in R^{D+S+E}$, we define $l = D+S+E$. Then the objective function (8) can be rewritten as follows.

$$\begin{aligned}\min \sum_{t=\tau}^{\tau+w} \hat{h}_t(P_{d,t}, P_{s,t}, P_{e,t}, P_{r,t}, P_{l,t}) + \sum_{d=1}^{D} \eta |P_{d,t} - P_{d,t-1}| \\ + \sum_{s=1}^{S} \varsigma |P_{s,t} - P_{s,t-1}| + \sum_{e=1}^{E} \iota |P_{e,t} - P_{e,t-1}| \qquad (18) \\ \text{s.t.: } \varsigma = 0, \iota = 0, \tau \in \Psi_m.\end{aligned}$$

Problem (18) has the same solution as problem (8).

We then transform (18) to a continuous, differentiable convex function as in Section III-A. We have

$$\begin{aligned}\min \sum_{t=\tau}^{\tau+w} \|P_{net,t} - A(\mu + \upsilon)\|_2^2 \qquad (19) \\ + \sum_{n=1}^{l} \varepsilon(\mu_n - \upsilon_n - (\mu_{n-1} - \upsilon_{n-1})) \\ \text{s.t.: } \mu_n - \mu_{n-1} \geq 0, \upsilon_n - \upsilon_{n-1} \leq 0, \tau \in \Psi_m,\end{aligned}$$

where $\varepsilon = [\eta, \varsigma, \iota]^T$ and A is the same as that in (14).

Assume (μ^*, υ^*) is the optimal solution to problem (19). Then $(\mu^{*'}, \upsilon^{*'}) = ((\mu^* + \upsilon^*)^+, (\mu^* + \upsilon^*)^-)$ is also optimal to (19), and it satisfies constraint $\mu^* \upsilon^* = 0$, for all n. For the case $\varepsilon_n > 0$, according to LEMMA 2.1 in [29], we have

$$\begin{aligned}\sum_{t=\tau}^{\tau+w} \|P_{net,t} - A(\mu^{*'} + \upsilon^{*'})\|_2^2 + \sum_{n=1}^{l} \varepsilon_n(\chi_n^{*'} - \chi_{n-1}^{*'}) \\ \leq \sum_{t=\tau}^{\tau+w} \|P_{net,t} - A(\mu^* + \upsilon^*)\|_2^2 + \sum_{n=1}^{l} \varepsilon_n(\chi_n^* - \chi_{n-1}^*), \qquad (20)\end{aligned}$$

where $\chi_n^* = \mu_n^* - \upsilon_n^*$, $\chi_{n-1}^* = \mu_{n-1}^* - \upsilon_{n-1}^*$, $\chi_n^{*'} = \mu_n^{*'} - \upsilon_n^{*'}$, and $\chi_{n-1}^{*'} = \mu_{n-1}^{*'} - \upsilon_{n-1}^{*'}$. This result contradicts the assumption. Therefore (μ^*, υ^*) is a feasible solution to problem (18). It is also the solution to problem (8). ■

APPENDIX B
CONVEX RELAXATION

We introduce the auxiliary variable for active power as ξ and $\xi \in R^{2D+S+E}$. For every element ξ_i in ξ, we have $\xi_i = 1$ and $\xi_i^2 = 1$. In the same manner, the auxiliary variable corresponding to the reactive power is described as γ and $\gamma \in R^K$, for each γ_i in γ, it satisfies $\gamma_i = 1$, then $\gamma_i^2 = 1$. Then we introduce auxiliary variables $[\Omega, \omega, \Delta, \delta, \Lambda, \zeta] \in R^M$, where $M = 4D + 2S + 2E + 2B$, to convert the non-convex

constraints to convex. The transformed objective function and constraints are as follows.

(i) Converted objective function

$$\min \sum_{t=\tau}^{\tau+w} \{ P_{net,t}^2 + (\rho_{d,t}\mu_{d,t} + \rho_{d,t}\upsilon_{d,t} + \rho_{s,t}P_{s,t} - P_{e,t})^2 - 2P_{net,t}(\rho_{d,t}\xi_{\mu d,t}\mu_{d,t} + \rho_{d,t}\xi_{vd,t}\upsilon_{d,t} + \rho_{s,t}\xi_{s,t}P_{s,t} - \xi_{e,t}P_{e,t}) + \sum_{d=1}^{D} \eta[\xi_{\mu d,t}\mu_{d,t} - \xi_{vd,t}\upsilon_{d,t} - (\xi_{\mu d,t-1}\mu_{d,t-1} - \xi_{vd,t-1}\upsilon_{d,t-1})]\} . \quad (21)$$

(ii) Converted constraints

$$\sum_{s=1}^{S}(\alpha_{s,t}P_{s,t}^2 + \Omega_{s,t}^2) = C_{s,t},\ \forall t \quad (22)$$

$$\sum_{d=1}^{D}(\alpha_{d,t}(\mu_{d,t} + \upsilon_{d,t})^2 + \beta(\xi_{\mu d,t}\mu_{d,t} + \xi_{vd,t}\upsilon_{d,t}) + \Omega_{\mu d,t}^2 + \Omega_{vd,t}^2) = C_{d,t} - \sum_{d=1}^{D}\lambda_{d,t},\ \forall t \quad (23)$$

$$\xi_{g,i}P_{g,i} - \sum_{j\in\mathbb{B}}[e_i(e_jG_{ij} - f_jB_{ij}) + f_i(f_jG_{ij} + e_jB_{ij})] = P_{li},\ \forall t \quad (24)$$

$$\xi_{\mu d,i}\mu_{d,i} + \xi_{vd,i}\upsilon_{d,i} - \sum_{j\in\mathbb{B}}[e_i(e_jG_{ij} - f_jB_{ij}) + f_i(f_jG_{ij} + e_jB_{ij})] = P_{li},\ \forall t \quad (25)$$

$$\gamma_{k,i}Q_{k,i} - \sum_{j\in\mathbb{B}}[f_i(e_jG_{ij} - f_jB_{ij}) - e_i(f_jG_{ij} + e_jB_{ij})] = Q_{li},\ \forall t, \quad (26)$$

$$\xi_{\mu d,i}\mu_{d,i} + \xi_{vd,i}\upsilon_{d,i} + \Omega_{\mu d,i}^2 + \Omega_{vd,i}^2 = P_{d,i}^{max},\ \forall t \quad (27)$$

$$\xi_{\mu d,i}\mu_{d,i} + \xi_{vd,i}\upsilon_{d,i} - \omega_{\mu d,i}^2 - \omega_{vd,i}^2 = P_{d,i}^{min},\ \forall t \quad (28)$$

$$\xi_{vd,t}\upsilon_{d,t} - \xi_{vd,t-1}\upsilon_{d,t-1} + \Omega_{vd,t-1}^2 + \Omega_{vd,t}^2 = 0,\ \forall t \quad (29)$$

$$\xi_{\mu d,t}\mu_{d,t} - \xi_{\mu d,t-1}\mu_{d,t-1} - \omega_{\mu d,t-1}^2 - \omega_{\mu d,t}^2 = 0,\ \forall t \quad (30)$$

$$\xi_{g,i}P_{g,i} + \Omega_{g,i}^2 = P_{g,i}^{max},\ \forall t \quad (31)$$

$$\xi_{g,i}P_{g,i} - \omega_{g,i}^2 = P_{g,i}^{min},\ \forall t \quad (32)$$

$$\gamma_{k,i}Q_{k,i} + \Delta_{k,i}^2 = Q_{k,i}^{max},\ \forall t \quad (33)$$

$$\gamma_{k,i}Q_{k,i} - \delta_{k,i}^2 = Q_{k,i}^{min},\ \forall t \quad (34)$$

$$SoC_{s,t} = SoC_{s,t-1} - \eta_s\xi_{s,t}P_{s,t},\ \forall t \quad (35)$$

$$\sum_{t=\tau}^{\tau+w}(P_{s,t} + \Omega_{s,t}^2) = SoC_0 - SoC_s^{min},\ \forall t \quad (36)$$

$$\sum_{t=\tau}^{\tau+w}(P_{s,t} - \omega_{s,t}^2) = SoC_0 - SoC_s^{max},\ \forall t \quad (37)$$

$$e_{ref}^2 = e_0^2,\ \forall t \quad (38)$$

$$f_{ref}^2 = f_0^2,\ \forall t \quad (39)$$

$$e_i^2 + f_i^2 + \Lambda_i^2 = (V_i^{max})^2,\ \forall t \quad (40)$$

$$e_i^2 + f_i^2 - \zeta_i^2 = (V_i^{min})^2,\ \forall t \quad (41)$$

$$\xi_i^2 = 1,\ \forall t \quad (42)$$

$$\gamma_i^2 = 1,\ \forall t, \quad (43)$$

for $g \in \mathbb{G}/\mathbb{D}, i \in \mathbb{B}, d \in \mathbb{D}, k \in \mathbb{K}, s \in \mathbb{S}$. SoC_0 is the initial state of the ESS in the MG, where $SoC_s^{min} \leq SoC_0 \leq SoC_s^{max}$. In this way, linear term variable in the classical OPF problem is reformulated into the quadratic terms, such as $P_{g,i}$ to $\xi_{g,i}P_{g,i}$, and by bringing auxiliary variable into inequality constraints, the classical OPF problem is equivalently converted to a quadratic problem with positive semidefinite constraints and variables [27], [28], [30]. Thus, the non-convex set is transformed into a convex set, and the original problem (8) is transformed into an SDP problem, which is easier to solve.

REFERENCES

[1] X. Wang, X. Wang, and S. Mao, "RF sensing for Internet of Things: A general deep learning framework," *IEEE Communications Magazine*, vol.56, no.9, pp.62–67, Sept. 2018.

[2] D. Giusto, A. Iera, G. Morabito, and L. Atzori, *The Internet of Things*. New York, US: Springer Press, 2010.

[3] L. Atzori, A. Iera, and G. Morabito, "The Internet of Things: A survey," *Elsevier Comput. Netw.*, vol. 54, pp.2787–2805, May 2010.

[4] Q. Yang, D. Li, W. Yu, Y. Liu, D. An, X. Yang, and J. Lin, "Toward Data Integrity Attacks Against Optimal Power Flow in Smart Grid," *IEEE Internet of Things J.*, vol. 4, no. 5, pp.1726–1738, Oct. 2017.

[5] Y. Wang, S. Mao and R. M. Nelms. *Online Algorithms for Optimal Energy Distribution in Microgrids*. New York, NY: Springer International Publishing, 2015.

[6] J. A. Stankovic, "Research Directions for the Internet of Things," *IEEE Internet of Things J.*, vol. 1, no. 1, pp.3–9, Feb. 2014.

[7] J. Lin, W. Yu, N. Zhang, X. Yang, H. Zhang, and W. Zhao, "A Survey on Internet of Things: Architecture, Enabling Technologies, Security and Privacy, and Applications," *IEEE Internet of Things J.*, vol. 4, no. 5, pp.1125–1142, Oct. 2017.

[8] T. Chiu, Y. Shih, A. Pang, and C. Pai, "Optimized day-ahead pricing with renewable energy demand-side management for smart grids," *IEEE Internet of Things J.*, vol. 4, no. 2, pp.374–383, Apr. 2017.

[9] F. Katiraei, R. Iravani, N. Hatziargyriou, and A. Dimeas. "Microgrids management," *IEEE Power & Energy Society Mag.*, vol. 6, no. 3, pp.54–65, May/June 2008

[10] X. Fang, S. Misra, G. Xue, and D. Yang, "Smart grid - the new and improved power grid: A survey," *IEEE Commun. Surv. & Tut.*, vol. 14, no. 4, pp.944–980, Fourth Quarter, 2012.

[11] V. Bui, A. Hussain, N. Kato, and H. Kim, "A multiagent-based hierarchical energy management strategy for multi-microgrids considering adjustable power and demand response," *IEEE Trans. Smart Grid*, vol. 9, no. 2, pp.1323–1333, Mar. 2018.

[12] A. M. Jadhav and N. R. Patne, "Priority-based energy scheduling in a smart distributed network with multiple microgrids," *IEEE Trans. Ind. Informat.*, vol. 13, no. 6, pp.3134–3143, Dec. 2017.

[13] N. Tang, S. Mao, Y. Wang, and R.M. Nelms, "Solar power generation forecasting with a LASSO-based approach," *IEEE Internet of Things J.*, vol.5, no.2, pp.1090–1099, Apr. 2018.

[14] Y. Wang, Y. Shen, S. Mao, G. Cao, and R. M. Nelms, "Adaptive learning hybrid model for solar intensity forecasting," *IEEE Trans. Ind. Informat.*, vol. 14, no. 4, pp.1635–1645, Apr. 2018.

[15] R. Palma-Behnke, C. Benavides, E. Aranda, J. Llanos, and D. Sez, "Energy management system for a renewable based microgrid with a demand side management mechanism," in *Proc. IEEE Symp. Comput. Intell. Appl. Smart Grid*, Paris, France, Apr. 2011, pp.1–8.

[16] W. Su, J. Wang, and J. Roh, "Stochastic energy scheduling in microgrids with intermittent renewable energy resources," *IEEE Trans. Smart Grid*, vol. 5, no. 4, pp.1876–1883, July 2014.

[17] H. Farzin, M. Fotuhi-Firuzabad, and M. Moeini-Aghtaie, "A stochastic multi-objective framework for optimal scheduling of energy storage systems in microgrids," *IEEE Trans. Smart Grid*, vol. 8, no. 1, pp.117–127, July 2017.

[18] Y. Wang, Y. Shen, S. Mao, and X. Chen, "LASSO & LSTM integrated temporal model for short-term solar intensity forecasting," *IEEE Internet of Things Journal*, revised, Oct. 2018.

[19] Y. Wang, S. Mao, and R. M. Nelms, "On hierarchical power scheduling for the macrogrid and cooperative microgrids," *IEEE Trans. Ind. Inform.*, vol. 11, no. 6, pp.1574–1584, Dec. 2015.
[20] R. Palma-Behnke, C. Benavides, F. Lanas, B. Severino, L. Reyes, J. Llanos, and D. Sez. "A microgrid energy management system based on the rolling horizon strategy," *IEEE Trans. Smart Grid*, vol. 4, no. 2, pp. 996–1006, Jan. 2013.
[21] Y. Wang, S. Mao, and R. M. Nelms, "Distributed online algorithm for optimal real-time energy distribution in smart grid," *IEEE Internet of Things*, vol. 1, no. 1, pp.70–80, Feb. 2014.
[22] J. Silvente, G. M. Kopanos, E. N. Pistikopoulos, and A. Espua, "A rolling horizon optimization framework for the simultaneous energy supply and demand planning in microgrids," *Elsevier Applied Energy*, vol. 155, pp.485–501, Oct. 2015.
[23] S. Moghadasi and S. Kamalasadan, "Optimal fast control and scheduling of power distribution system using integrated receding horizon control and convex conic programming," *IEEE Trans. Ind. Appl.*, vol. 52, no. 3, pp.2596–2606, May/June 2016.
[24] N. Chen, A. Agarwal, A. Wierman, S. Barman, and L. L. H. Andrew, "Online convex optimization using predictions," *ACM Sigmetrics Performance Evaluation Review*, vol. 43, no. 1, pp.191–204, June 2015.
[25] M. Lin, Z. Liu, A. Wierman, and L. L. H. Andrew, "Online algorithms for geographical load balancing," *Proc. Green Computing Conf.*, San Jose, CA, June 2012, pp. 1–10.
[26] S. Kim, K. Koh, M. Lustig, S. Boyd, and D. Gorinevsky, "An interior-point method for large-scale l1-regularized least squares," *IEEE J. Sel. Topics Signal Process.*, vol. 1, no. 4, pp.606–617, Dec. 2007.
[27] S. H. Low, "Convex relaxation of optimal power flow–Part I: Formulations and equivalence," *IEEE Trans. Control Netw. Syst.*, vol. 1, no. 1, pp.15–27, Mar. 2014.
[28] D. K. Molzahn, F. Drfler, H. Sandberg, S. H. Low, S. Chakrabarti, R. Baldick, and J. Lavaei, "A Survey of Distributed Optimization and Control Algorithms for Electric Power Systems," *IEEE Trans. Smart Grid*, vol. 8, no. 6, pp.2941–2962, Nov. 2017.
[29] T. Wu, Y. Chu, and Y. Yu, "On solving Lq-penalized regressions," *Adv. Decis. Sci.*, vol. 2007, Article ID 24053, pp.1–13, 2007.
[30] X. Bai, H. Wei, K. Fujisawa, and Y. Wang, "Semidefinite programming for optimal power flow problems," *Electrical Power & Energy Systems*, vol. 30, no. 6/7, pp.383–392, July/Sept. 2008.
[31] Y. Huang and S. Mao, "On Quality of Usage provisioning for electricity scheduling in microgrids," *IEEE Systems J.*, vol. 8, no. 2, pp.619–628, June 2014.
[32] Y. Wang, S. Mao, and R. M. Nelms, "An online algorithm for optimal real-time energy distribution in smart grid," *IEEE Trans. Emerging Topics Comput.*, vol. 1, no. 1, pp.10–21, July 2013.
[33] H. Wang, and J. Huang, "Incentivizing energy trading for interconnected microgrids," in *IEEE Trans. Smart Grid*, vol. 9, no. 4, pp.2647–2657, July 2018.
[34] M. Badiei, N. Li, and A. Wierman "Online convex optimization with ramp constraints," in *Proc. IEEE CDC'15*, Osaka, Japan, Dec. 2015, pp.6730–6736.
[35] W. Shi, N. Li, C. Chu, and R. Gadh, "Real-time energy management in microgrids," in *IEEE Trans. Smart Grid*, vol. 8, no. 1, pp.228–238, Jan. 2017.
[36] S. R. Cominesi, M. Farina, L. Giulioni, B. Picasso, and R. Scattolini, "A two-layer stochastic model predictive control scheme for microgrids," *IEEE Trans. Control Syst. Tech.*, vol. 26, no. 1, pp.1–13, Jan. 2018.
[37] S. J. Chung, and K. G. Murty, "Polynomially bounded ellipsoid algorithms for convex quadratic programming," *Nonlinear Programming*, vol. 4, pp.439–458, 1981.
[38] S.Matsuyama, K. Fujisawa, and K. Nakata, "SDPA-M (SemiDefinite Programming Algorithm in MATLAB) sser's manual - Version 1.00," [online] Available: www.is.titech.ac.jp/~kojima/articles/B-359.pdf, accessed on Aug. 9, 2018.
[39] R. Zimmerman and C. Murillo-Snchez, "MATPOWER 6.0 User's Manual," *Power Systems Engineering Research Center*, [online] Available: http://www.pserc.cornell.edu/matpower/docs/MATPOWER-manual-6.0.pdf, accessed on Aug. 9, 2018.

Hualei Zou [S'18] received the B.E. degree in Electrical Engineering and Automation from Nanjing University of Aeronautics and Astronautics (NUAA), Nanjing, China in 2008 and M.E. degree in Power Electronics and Power Drives from Jiangsu University, Zhenjiang, China in 2011. Since 2014, she has been pursuing the Ph.D. degree in the Department of Electrical Engineering, NUAA, Nanjing, China. Her research interests include energy management in Smart Grid and Microgrid, Optimization.

Yu Wang [S'13-M'17] received the B.S and M.S. degrees in instrument and meter engineering from Southeast University, Nanjing, China in 2008 and 2011, respectively. He received Ph.D. in electrical and computer engineering from Auburn University, Auburn, AL, in 2015. Currently, he is an Assistant Professor in the Department of Electrical Engineering, Nanjing University of Aeronautics and Astronautics, Nanjing, China. His research interests include smart grid, microgrid, renewable energy power forecasting, management, and optimization.

Shiwen Mao [S'99-M'04-SM'09] is the Samuel Ginn Distinguished Professor and Director of the Wireless Engineering Research and Education Center at Auburn University, Auburn, AL. His research interests include wireless networks and multimedia communications. He is a Distinguished Speaker of the IEEE Vehicular Technology Society. He is on the Editorial Board of IEEE Internet of Things Journal, IEEE Transactions on Mobile Computing, IEEE Transactions on Multimedia, IEEE Multimedia, ACM GetMobile, among others. He is a co-recipient of the 2004 IEEE Communications Society Leonard G. Abraham Prize in the Field of Communications Systems.

Fanghua Zhang received the B.S. degree in automation and electrical engineering from Jinan University, Jinan, China, in 1999, and the Ph.D. degrees in electrical engineering from Nanjing University of Aeronautics and Astronautics (NUAA), Nanjing, China in 2004. He joined the College of Automation Engineering,NUAA, in June 2004, as a Lecturer and became an Associate Professor in March 2006. His research focuses on dc-dc converter, high-performance aeronautical static inverter for aerospace applications, and power electronic systems stability and power quality.

Xin Chen [S'99-M'04] received the B.S. and Ph.D. degrees in electrical engineering from the Nanjing University of Aeronautics and Astronautics, Nanjing, China, in 1996 and 2001, respectively. From 2001 to 2003, he was a Chief Engineer with the Power Division of ZTE Corporation. From 2010 to 2011, he was an Invited Researcher with the Rensselaer Polytechnic Institute, Troy, USA. He is currently an Associate Professor at the Nanjing University of Aeronautics and Astronautics. His current research interests include power electronic converters, distributed generation, and microgrids.